

# Spin-torque driven ferromagnetic resonance of Co/Ni synthetic layers in spin valves

W. Chen, J-M. L. Beaujour, G. de Loubens, A. D. Kent  
*Department of Physics, New York University, New York, NY 10003*

J. Z. Sun

*IBM T. J. Watson Research Center, Yorktown Heights, NY 10598*

(Dated: November 30th, 2007)

Spin-torque driven ferromagnetic resonance (ST-FMR) is used to study thin Co/Ni synthetic layers with perpendicular anisotropy confined in spin-valve based nanojunctions. Field swept ST-FMR measurements were conducted with a magnetic field applied perpendicular to the layer surface. The resonance lines were measured under low amplitude rf excitation, from 1 to 20 GHz. These results are compared with those obtained using conventional rf field driven FMR on extended films with the same Co/Ni layer structure. The layers confined in spin valves have a lower resonance field, a narrower resonance linewidth and approximately the same linewidth *vs* frequency slope, implying the same damping parameter. The critical current for magnetic excitations is determined from measurements of the resonance linewidth *vs* dc current and is in accord with the one determined from I-V measurements.

Spin-transfer torque has been theoretically predicted and experimentally demonstrated to drive magnetic excitations in nanostructured spin valves and magnetic tunnel junctions [1, 2, 3, 4, 5]. With an rf current, spin transfer can be used to study ferromagnetic resonance [6, 7]. This technique, known as spin-torque driven ferromagnetic resonance (ST-FMR), enables quantitative studies of the magnetic properties of thin layers in a spin-transfer device. Specifically, the layer magnetic anisotropy and damping can be determined [8], which are important parameters that need to be optimized in spin-torque-based memory and rf oscillator applications.

Spin-transfer memory devices will likely include magnetic layers with perpendicular magnetic anisotropy that counteracts their shape-induced easy-plane anisotropy. This will allow efficient use of spin current for magnetic reversal with a reduced switching threshold [9] and a faster switching process [10]. Recent work by Mangin *et al.* [11] has demonstrated improvements of spin-torque efficiency in a spin valve that has perpendicularly magnetized Co/Ni synthetic layers. For further optimization of perpendicular anisotropy materials, it is important to have quantitative measurements of their anisotropy field and damping in a nanostructured device, as both of these parameters directly affect the threshold current for spin-transfer induced switching.

In this Letter, we present ST-FMR studies of bilayer nanopillars, where the thin (free) layer is composed of a Co/Ni synthetic layer and the thick (fixed) layer is pure Co. The magnetic anisotropy and damping of the Co/Ni have been determined by ST-FMR. We compare these results with those obtained from extended films with the same Co/Ni layer stack measured using traditional rf field driven FMR.

Pillar junctions with submicron lateral dimensions (Fig. 1(a)) were patterned on a silicon wafer using a nanostencil process [12]. Junctions were deposited using metal evaporation with the layer structure || 1.5 nm

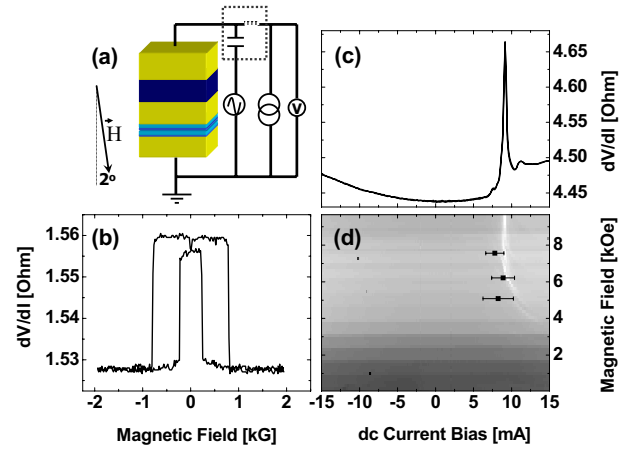


FIG. 1: (a): Sample layer structure and ST-FMR circuit. (b): Zero current in-plane MR hysteresis loop for a  $50 \times 150$  nm<sup>2</sup> spin valve junction with  $t=0.4$ . (c):  $dV/dI$  vs  $I$  of the same junction with a perpendicular magnetic field of 9.5 kOe. (d): Contour plot of  $dV/dI$  as a function of both dc current and perpendicular magnetic field. Data points: critical currents determined from ST-FMR at three different fields and frequencies (see text).

Cr| 100 nm Cu| 20 nm Pt| 10 nm Cu| [ $t$  nm Co|  $2t$  nm Ni]  $\times$  1.2/ $t$  | 10 nm Cu| 12 nm Co| 200 nm Cu||. We varied the Co thickness  $t$  from 0.1 to 0.4, tuning the magnitude of the Co/Ni composite layer's net anisotropy, while keeping the total magnetic moment and thickness of the free layer constant. For ST-FMR measurements, an rf current generated by a high frequency source is added to a dc current using a bias-T (the dashed-line box in Fig. 1(a)). Positive dc currents are defined such that electrons flow from the free layer to the fixed layer.

The magnetoresistance (MR) was measured with a magnetic field applied in the film plane using a 4-point

geometry. A typical MR hysteresis loop of a  $50 \times 150 \text{ nm}^2$  junction with  $t=0.4$  is shown in Fig. 1(b). The magnetoresistance  $\text{MR} = (R_{AP} - R_P)/R_P$  is  $\simeq 2.3 \pm 0.3 \%$  for all junctions, independent of  $t$ , within the range investigated. Here  $R_{AP}$  ( $R_P$ ) represents the static junction resistance when the free layer and fixed layer magnetizations are antiparallel (parallel). Current-voltage measurements were conducted with a magnetic field applied *nearly* perpendicular to the sample surface (The field was applied  $2^\circ$  from the film normal to produce a small in-plane field along the easy axis of the junction. This was done to suppress vortex states in the magnetic layers.) Measurements were conducted in a 2-point geometry where lead resistances are included. Fig. 1(c) shows  $dV/dI$  vs  $I$  of the same junction in a 9.5 kOe applied field. A peak without hysteresis is observed at 9.1 mA, which we interpret as the critical current  $I_C$  for excitation of the free layer [13]. A contour plot of 2-point  $dV/dI$  as the function of both current and perpendicular magnetic field is shown in Fig. 1(d). The peak in  $dV/dI$  is seen as the bright color at high field and current.

At resonance, the rf current and spin valve resistance oscillate at the same frequency resulting in a dc voltage ( $V = \langle I(t)R(t) \rangle$ ) [6, 7]. This voltage can be expressed as  $V = \frac{1}{4}(R_{AP} - R_P)I_{\text{rf}} \sin \beta \sin \theta$ . Here  $\beta$  is the angle between the free and fixed layers before applying the rf current and  $\theta$  is the precession angle.  $I_{\text{rf}}$  represents the rf current amplitude. This is a simplified formula that assumes small angle precession and a sinusoidal angular dependence of junction resistance between parallel and antiparallel states. With a perpendicular magnetic field greater than the free layer's easy-plane anisotropy field, the free layer magnetization is normal to the surface, while the fixed layer, which has a larger easy-plane anisotropy field, is still mainly magnetized in the film plane. This non-collinear arrangement of the layer magnetizations ( $\beta \lesssim \pi/2$ ) enhances the ST-FMR signal. To further increase the signal (typically in the sub- $\mu\text{V}$  range) to noise ratio, we modulate the rf current on and off at 800 Hz and use a lock-in amplifier to detect the voltage at this frequency.

ST-FMR measurements were conducted with the circuit shown in Fig. 1(a). Resonance lines under low amplitude rf current at zero dc current and different rf frequencies  $f$  are plotted in Fig. 2(a) versus perpendicular magnetic field. Different frequencies (3~20 GHz in 1 GHz steps) are plotted with each adjacent curve offset by 0.4  $\mu\text{V}$ . The voltage signals are shown on the left vertical axis. From the peak height  $V_{\text{peak}}$  and  $I_{\text{rf}}$ , we estimate the precession angle to be  $\sim 4^\circ$ . We verified that this set of data was taken in a linear response regime with  $V_{\text{peak}}/I_{\text{rf}}^2$  independent of  $I_{\text{rf}}$ . These data are typical of all junctions with  $t=0.4$ . However, much broader resonance peaks and multiple peaks were found on samples with  $t=0.1, 0.2$  and  $0.3$ . This is likely associated with the excitation of higher order spin wave modes, but is not presently understood. Therefore, data analysis and discussion mainly focus on samples with  $t=0.4$ .

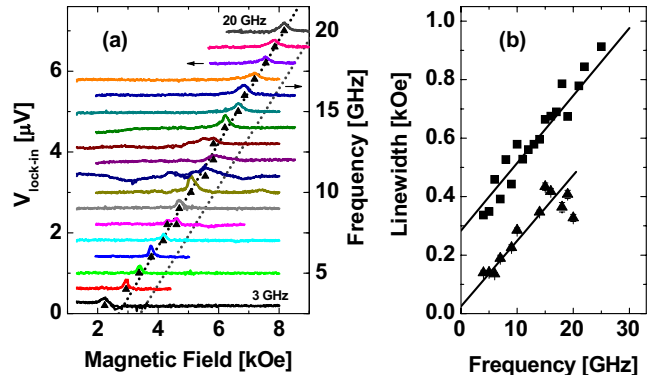


FIG. 2: (a): Lock-in voltage signal as a function of applied perpendicular magnetic field at different rf frequencies from 3 up to 20 GHz in 1 GHz steps.  $\blacktriangle$ :  $H_{\text{res}}$  of a  $50 \times 150 \text{ nm}^2$ ,  $t=0.4$  Co/Ni synthetic free layer in a spin valve; black dashed line: corresponding linear fit; gray dashed line: a linear fit of  $H_{\text{res}}$  vs  $f$  of an extended film with the same Co/Ni layer stack. (b):  $\Delta H$  vs  $f$  for the spin valve junction ( $\blacktriangle$ ) and the extended film ( $\blacksquare$ ), together with their corresponding linear fits.

We also measured resonance lines on an extended film with the same Co/Ni synthetic layer stack sandwiched between 10 nm Cu on each side. These measurements were conducted with a traditional rf field driven FMR using a flip-chip method [14]. Broader resonance peaks were not found in extended films with  $t=0.1, 0.2$ , and  $0.3$ .

The resonance field  $H_{\text{res}}$  of the Co/Ni element in the spin valve increases linearly with  $f$  above 4 GHz, as shown in Fig. 2(a) ( $\blacktriangle$  symbols). At lower frequencies, the free layer magnetization tilts into the plane, leading to a lower resonance field. A linear fit of  $H_{\text{res}}$  vs  $f$  of the extended film is also plotted with a gray dashed line (to the right of the  $\blacktriangle$  symbols) in Fig. 2(a). A linear relationship between  $f$  and  $H_{\text{res}}$  in extended magnetic films is expected when the magnetization is normal to the film surface  $\frac{\hbar}{\mu_B} f = g(H_{\text{res}} - 4\pi M_{\text{eff}})$  [15]. Here  $g$  is the Landé  $g$  factor and the easy-plane anisotropy is  $4\pi M_{\text{eff}} = 4\pi M_s - H_P$ , where  $M_s$  and  $H_P$  represent the saturation magnetization and the perpendicular anisotropy field. A linear fit of each data set (dashed lines in Fig. 2(a)) gives  $g=2.17$  and  $4\pi M_{\text{eff}} = 2.58 \text{ kOe}$  for the extended film, and a slightly larger slope (2.28) and a smaller field-axis intercept (1.92 kOe) for the Co/Ni element confined in the spin valve. This consistency between data sets confirms that the main peak of the ST-FMR signal is associated with the Co/Ni synthetic free layer rather than the other magnetic layers. The differences are associated with the static dipolar fields from other magnetic layers and finite size effects on the spin wave modes, which is discussed in detail in a forthcoming

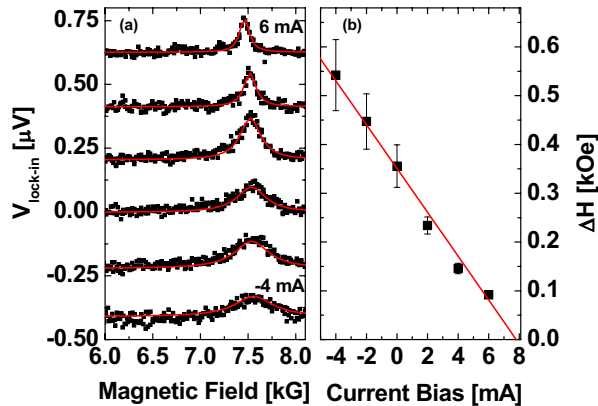


FIG. 3: (a): ST-FMR signal as a function of applied field at different dc currents. The rf frequency was set at 18 GHz, and the rf amplitudes were 595, 595, 470, 470, 315 and 315  $\mu\text{A}$  respectively for each dc current from -4 to 6 mA in 2 mA steps. Each adjacent curve is offset by  $0.20 \mu\text{V}$ . Solid lines are Lorentzian fits of each data set. (b):  $\Delta H$  (full width at half maximum) *vs* dc current.

publication [16].

Here we focus on the resonance linewidth  $\Delta H$ .  $\Delta H$  *vs*  $f$  at zero dc bias is plotted in Fig. 2(b).  $\Delta H$  of both the Co/Ni layer in spin valve ( $\blacktriangle$ ) and the same-stack extended film ( $\blacksquare$ ) increases linearly with  $f$ . Linear fits are shown as solid lines in Fig. 2(b), and give an intercept and slope:

$$\Delta H = \Delta H_0 + \frac{2\alpha h}{g\mu_B} f \quad (1)$$

where  $h$  is the Planck Constant and  $\mu_B$  is the Bohr Magneton. The first term  $\Delta H_0$  describes the inhomogeneous broadening, and the second term is related to the damping  $\alpha$  [17].  $\Delta H$  *vs*  $f$  of the spin valve and that of the extended film have a similar slope, implying a similar damping parameter ( $\alpha=0.036\pm 0.002$  for the extended film and  $0.033\pm 0.003$  for the magnetic layer in the spin valve). However, the intercepts are quite different:  $\Delta H_0=24\pm 15$  Oe in the spin valve, which is much lower than that of the extended film,  $284\pm 30$  Oe.

When a dc current bias is applied to a spin-valve, there is an additional spin transfer torque that modifies the free layer's effective damping,  $\alpha_{\text{eff}} = \alpha(1 - \frac{I}{I_c})$ , where  $I$  is the dc current. Thus  $\alpha_{\text{eff}}$  decreases with increasing positive current up to a critical current  $I_c$ , that defines the threshold for magnetic excitation of the free layer. The critical current in the Slonczewski model [1] is given by  $I_c = \frac{2e}{\hbar P} \frac{\alpha M_s V}{\cos\beta} (H - 4\pi M_{\text{eff}})$ , where  $P$  is the spin po-

larization factor and  $V$  is the volume of the magnetic element. So with a dc bias,  $\Delta H - \Delta H_0 = \frac{2\alpha h f}{g\mu_B} (1 - \frac{I}{I_c})$ , and therefore at fixed frequency  $\Delta H - \Delta H_0$  depends linearly on current and goes to zero at the critical current. We plot resonance lines of the spin valve with  $f = 18$  GHz at different dc currents from -4 to 6 mA in 2 mA steps in Fig. 3(a).  $\Delta H$  *vs* dc current bias is shown in Fig. 3(b). The intercept of  $\Delta H$  *vs*  $I$  is 7.8 mA. Inclusion of  $\Delta H_0$  decreases the intercept by no more than 0.2 mA, because  $\Delta H_0$  is small compared to the linewidth at the dc currents studied. Critical currents determined for  $f = 10, 14$  and 18 GHz are plotted in Fig. 1(d), and agree well with those obtained from the I-V measurements. Further,  $I_c$  is quantitatively consistent with the Slonczewski model taking a spin polarization factor  $P \sim 0.3$ .

The frequency independent term  $\Delta H_0$  originates from film inhomogeneities: roughness, polycrystalline structure, as well as defects. The scale of the inhomogeneities is likely the film grain size,  $5\sim 10$  nm. In a simple model, fluctuations in  $H_{\text{res}}$  from grain to grain result in an inhomogeneously broadened resonance line [18]. However, it is likely that the exchange coupling between grains is important to a detailed understanding of the linewidth [19].

The free layer in the nanostructured device contains at most a few hundred grains, therefore one expects less inhomogeneity than that in extended film. More importantly, the lateral magnetic confinement results in strongly varying internal field in the plane of the nanostructure that lifts the degeneracy between different spin wave modes. Numerical and analytical calculations of normal modes in the Co/Ni rectangular element are presented and compared with our ST-FMR data in Ref. [16]. The separation between them is more than the inhomogeneous broadening  $\Delta H_0$  in the extended film, therefore we expect that the linewidth measured on an individual mode is close to its intrinsic value (the term proportional to  $f$  in Eq. 1) [20]. The remaining inhomogeneous broadening in the nanostructure may be attributed to the quasi-degeneracy subsisting between some very closely spaced modes resulting from film inhomogeneities.

In summary, ST-FMR has been used to study the magnetic properties of Co/Ni synthetic layers with perpendicular anisotropy in spin valves. The ST-FMR resonance lines were compared with those of traditional FMR on same-stack extended film. The damping of the ST-device free layer is essentially the same as that of an unpatterned film and the critical currents determined from the ST-FMR homogeneous linewidth are in agreement with those of quasistatic I-V measurements.

This research is supported by NSF-DMR-0706322 and an NYU-Research Challenge Fund award.

[1] J. C. Slonczewski, J. Magn. Magn. Mater. **159**, L1 (1996).

[2] L. Berger, Phys. Rev. B **54**, 9353 (1996).

- [3] J. A. Katine, F. J. Albert, R. A. Buhrman, E. B. Myers, and D. C. Ralph, *Phys. Rev. Lett.* **84**, 3149 (2000).
- [4] J. Z. Sun, *J. Magn. Magn. Mater.* **202**, 157 (1999).
- [5] Y. Huai, F. Albert, P. Nguyen, M. Pakala, and T. Valet, *Appl. Phys. Lett.* **84**, 3118 (2004).
- [6] A. A. Tulapurkar, Y. Suzuki, A. Fukushima, H. Kubota, H. Maehara, K. Tsunekawa, D. D. Djayaprawira, N. Watanabe, and S. Yuasa, *Nature* **438**, 339 (2005).
- [7] J. C. Sankey, P. M. Braganca, A. G. F. Garcia, I. N. Krivorotov, R. A. Buhrman, and D. C. Ralph, *Phys. Rev. Lett.* **96**, 227601 (2006).
- [8] G. D. Fuchs, J. C. Sankey, V. S. Pribiag, L. Qian, P. M. Braganca, A. G. F. Garcia, E. M. Ryan, Z.-P. Li, O. Ozatay, D. C. Ralph, and R. A. Buhrman, *Appl. Phys. Lett.* **91**, 062507 (2007).
- [9] J. Z. Sun, *Phys. Rev. B* **62**, 570 (2000).
- [10] A. D. Kent, B. Özyilmaz, and E. del Barco, *Appl. Phys. Lett.* **84**, 3897 (2004).
- [11] S. Mangin, D. Ravelosona, J. A. Katine, M. J. Carey, B. D. Terris, and E. E. Fullerton, *Nature Materials* **5**, 210 (2006).
- [12] J. Z. Sun, *Appl. Phys. Lett.* **81**, 2202 (2002).
- [13] B. Özyilmaz, A. D. Kent, D. Monsma, J. Z. Sun, M. J. Rooks, and R. H. Koch, *Phys. Rev. Lett.* **91**, 067203 (2003).
- [14] J.-M. Beaujour, W. Chen, K. Krycka, C.-C. Kao, J. Z. Sun, and A. D. Kent, *Eur. Phys. J. B* **59**, 475 (2007).
- [15] C. Kittel, *Introduction to Solid State Physics* (John Wiley & Sons, Inc., New York, 1996).
- [16] W. Chen, G. de Loubens, J.-M. L. Beaujour, A. D. Kent, and J. Z. Sun, to be published in *J. Appl. Phys.* as MMM'07 Conference Proceeding, preprinted at arXiv:0712.0404 (2007).
- [17] D. L. Mills and S. M. Rezende, *Spin Dynamics in Confined Magnetic Structures II* (Springer, Heidelberg, 2002).
- [18] H. Hurdequint, *J. Magn. Magn. Mater.* **242-245**, 521 (2002).
- [19] R. D. McMichael, D. J. Twisselmann, and A. Kunz, *Phys. Rev. Lett.* **90**, 227601 (2003).
- [20] G. de Loubens, V. V. Naletov, O. Klein, J. B. Youssef, F. Boust, and N. Vukadinovic, *Phys. Rev. Lett.* **98**, 127601 (2007).